Since January 2020 Elsevier has created a COVID-19 resource centre with free information in English and Mandarin on the novel coronavirus COVID-19. The COVID-19 resource centre is hosted on Elsevier Connect, the company's public news and information website.

Journal of Immunological Methods 424 (2015) 111–119

Contents lists available at ScienceDirect

Journal of Immunological Methods

journal homepage: www.elsevier.com/locate/jim

Research paper

Identification and characterisation of T-cell epitopes for incorporation into dendritic cell-delivered *Listeria* vaccines

Ricardo Calderon-Gonzalez [a], Raquel Tobes [b], Eduardo Pareja [b], Elisabet Frande-Cabanes [a], Nikolai Petrovsky [c,d], Carmen Alvarez-Dominguez [a,*]

[a] Grupo de Genómica, Proteómica y Vacunas, Instituto de Investigación Marqués de Valdecilla (IDIVAL), Santander, Spain
[b] Information Technologies Research Group, Era7 Bioinformatics, Granada, Spain
[c] Department of Diabetes and Endocrinology, Flinders University, Adelaide, Australia
[d] Vaxine Pty Ltd, Flinders Medical Center, Adelaide, Australia

ARTICLE INFO

Article history:
Received 3 April 2015
Received in revised form 25 May 2015
Accepted 26 May 2015
Available online 29 May 2015

Keywords:
Listeriosis
Dendritic cells
Vaccines
Listeriolysin O
Glyceraldehyde-3-phosfate-dehydrogenase

ABSTRACT

Dendritic cells loaded with antigenic peptides, because of their safety and robust immune stimulation, would be ideal for induction of immunity to protect against listeriosis. However, there is no currently accepted method to predict which peptides derived from the *Listeria* proteome might confer protection. While elution of peptides from MHC molecules after *Listeria* infection yields high-affinity immune-dominant epitopes, these individual epitopes did not reliably confer *Listeria* protection. Instead we applied bioinformatic predictions of MHC class I and II epitopes to generate antigenic peptides that were then formulated with Advax™, a novel polysaccharide particulate adjuvant able to enhance cross-presentation prior to being screened for their ability to induce protective T-cell responses. A combination of at least four intermediate strength MHC-I binding epitopes and one weak MHC-II binding epitope when expressed in a single peptide sequence and formulated with Advax adjuvant induced a potent T-cell response and high TNF-α and IL-12 production by dendritic cells resulting in robust listeriosis protection in susceptible mice. This T-cell vaccine approach might be useful for the design of vaccines to protect against listeriosis or other intracellular infections.

1. Introduction

Dendritic cells (DCs) present antigenic peptides on MHC I and class II molecules resulting in stimulation of $CD8^+$ and $CD4^+$ T cells, respectively. This ability to activate both CD4 and CD8 T cell responses is the basis for the effectiveness of DC-based vaccines in prophylaxis against infections including HIV, *Streptococcus pneumonia*, *Chlamydia trachomatis* or *Mycobacterium* (Vacas-Cordoba et al., 2013; Cohen et al., 2012; Rey-Ladino et al., 2014; Kawasaki et al., 2014; Fromen et al., 2015).

Groups at risk of listeriosis include pregnant women, neonates, the elderly and immune-compromised patients. DC vaccines loaded *ex vivo* with peptides and injected back into the host, are highly effective at inducing cellular immunity and thereby could be useful for *Listeria* immunization (Wood and Paterson, 2014).

The objective of this study was to find a simple method to predict the minimum epitope requirements for a DC vaccine against human listeriosis and involved testing DC vaccines in mice susceptible or resistant to *Listeria*. C57BL/6 mice have a *Listeria* resistant allele at the *Hc* locus on chromosome 2 and show reduced susceptibility to intravenous, *i.v.*, intragastric, *i.g.* or intraperitoneal, *i.p*, challenge with *Listeria* when compared to susceptible Balb/c mice (Mainou-Fowler et al., 1988; Poulsen et al., 2011). Therefore, we used C57BL/6 mice to mimic the population at low risk of listeriosis, while Balb/c mice were used to mimic high-risk groups. Two *Listeria* antigens were selected as the focus of our study, listeriolysin O (LLO) and the glyceraldehyde-3-phosphate-dehydrogenase (GAPDH) as they have previously been shown to elicit strong $CD4^+$ and $CD8^+$ T cell responses (Alvarez-Dominguez et al., 2008; Calderon-Gonzalez et al., 2014, 2015). This was important as human listeriosis is not well characterised and antigens other than LLO or GAPDH that induce cellular immunity have yet to be found (Angelakopoulos et al., 2002; CAD and RCG unpublished results).

Bioinformatic methods that predict T cell epitopes *via* their ability to bind MHC molecules provide a faster and less costly alternative to strategies for selection of T-cell vaccine candidates such as MHC peptide elution or assays to map T-cell epitopes using complete sets of overlapping peptides (Geginat et al., 2001; Skoberne and Geginat, 2002). This is

Abbreviations: DC, dendritic cell; GAPDH, glyceraldehyde-3-phosphate dehydrogenase; *i.p*, intra-peritoneal; LLO, listeriolysin O; MHC, major histocompatibility complex.

* Corresponding author at: Grupo de Genómica, Proteómica y Vacunas, Instituto de Investigación Marqués de Valdecilla (IDIVAL), Laboratorio 124, Edificio IDIVAL, Avda, Cardenal Herrera Oria, s/n. 39011 Santander, Cantabria, Spain.
E-mail address: calvarez@humv.es (C. Alvarez-Dominguez).

http://dx.doi.org/10.1016/j.jim.2015.05.009

especially relevant given the limited current data on *Listeria* epitopes (Yu et al., 2002).

Another challenge when developing T-cell vaccines is the restricted ability of soluble antigens to stimulate strong T-cell responses, which at least in part reflects the lack of MHC class I cross-presentation of such antigens. Hence to maximise T-cell responses against *Listeria* an adjuvant is needed to up-regulate presentation of antigen on MHC class I and class II molecules on the surface of antigen presenting cells. Advax™ is a novel polysaccharide adjuvant derived from microparticles of delta β-D-[2-1]poly(fructo-furanosyl)α-D-glucose (delta inulin) (Cooper and Petrovsky, 2011; Cooper et al., 2013, 2014, 2015). Advantages of Advax include the fact that it has already been shown to be well tolerated, effective and safe for human use (Gordon et al., 2012, 2014), but most importantly for the current study, its demonstrated ability to induce potent $CD4^+$ and $CD8^+$ T cell responses against a wide variety of exogenous antigens including proteins from Japanese encephalitis, influenza, hepatitis B, HIV, and SARS coronavirus (Lobgis et al., 2010; Cristillo et al., 2011; Saade et al., 2013; Honda-Okubo et al., 2015). Hence, Advax adjuvant had ideal properties for use in our *Listeria* T-cell epitope screening programme.

We present a method that combines bioinformatics and structural predictions of peptide binding to MHC class I and class II molecules with convenient T-cell readouts. Vaccine predictions were validated *in vivo* and immunological parameters checked to confirm vaccine efficiency.

2. Methods

2.1. Cells

Mice were 8–12 week-old female Balb/c from Charles River (France) or C57BL/6 from our animal facility. DCs were obtained from femur bone-marrow, differentiated with GM-CSF, and $CD11c^+$ cells isolated with anti-mouse CD11c-coated magnetic beads and MACS™ separation columns (Miltenyi Biotech Inc., Auburn, CA) (Kono et al., 2012; Calderon-Gonzalez et al., 2014). DCs used were $MHC\text{-}II^+CD11c^+CD40^+CD11b^{+/-}CD86^{+/-}F4/80^-Gr\text{-}1^-$.

2.2. Peptides and adjuvants

We used $GAPDH_{1-15}$, $GAPDH_{1-22}$, LLO_{91-99}, $LLO_{296-304}$, $LLO_{189-201}$, $LLO_{189-200}$ and $LLO_{190-201}$ peptides. Peptides were synthesized at CNB (CSIC, Madrid) followed by HPLC and mass spectrometry using a MALDI-TOF Reflex™ IV mass spectrometer (Bruker Daltonics, Bremen, Germany). Peptide purity was >95% after HPLC. Advax™ adjuvant (Adv1) was supplied by Vaxine (Adelaide, Australia) and was mixed with antigen by simple admixture immediately before immunization of mice or *in vitro* analysis.

2.3. Bacteria

Listeria monocytogenes 10403S strain (LM^{WT}) was obtained from D.A. Portnoy (University of California, Berkeley, CA, USA).

2.4. Preparation of peptide pulsed DC vaccines

Cultured DCs were *ex vivo* loaded with 50 μg/ml of $GAPDH_{1-15}$, $GAPDH_{1-22}$, LLO_{91-99}, $LLO_{296-304}$, $LLO_{189-200}$, $LLO_{190-201}$ or $LLO_{189-201}$ peptides for 24 h in the presence of 50 μg/ml of Advax. Supernatants were collected and stored at −80 °C for cytokine measurements. Cells were analysed for cell surface markers by FACS.

2.5. Measurement of viability and apoptosis

Cultured DCs were also analysed for viability incubating cells with Trypan-blue. Cells stained with Trypan-blue were considered dead cells, while cells non-stained with the dye were viable. Cells were counted in a Neubauer haemocytometer and results were expressed as the mean of the percentages of viable cells ± SD. DCs were also examined for apoptosis by FACS analysis after double staining with 7-AAD and annexin-V (BD-Biosciences). In brief, DCs were incubated with 7-AAD and annexin-V-APC for 60 min at 4 °C, washed and analysed by flow cytometry. Double negative cells correspond to cells non-permeable to any reagent and therefore alive (Q3 region). Cells positive for annexin-V but negative for 7-AAD corresponded to early apoptotic cells (Q4 region). Double positive cells for annexin-V and 7-AAD corresponded to late apoptotic cells (Q2 region) and cells negative for annexin-V but positive for 7-AAD correspond to necrotic cells (Q1 region). Results are expressed as the mean of the percentages of late apoptotic cells (L-apoptosis) or early apoptotic cells (E-apoptosis) ± SD.

2.6. T-cell responses elicited by DC-LLO or DC-GAPDH vaccines

For delayed type hypersensitivity (DTH) analysis, Balb/c and C57BL/6 mice immunised *i.p* with LM^{WT} (5×10^3 CFU) were inoculated 7 days later in left hind footpads with DC vaccines (10^6 cells/mice) in the presence or absence of Advax (50 μg/ml). Non-inoculated right hind footpads served as negative controls. Positive controls of this assay included DC pre-infected *in vitro* with wild type LM (DC-LM^{WT}) as previously reported (Calderon-Gonzalez et al., 2015). After 24 h, we measured the footpad thickness with a calliper. T cell results in the footpads are expressed in millimetres as the mean of three different experiments ± SD.

2.7. Vaccination protocols

Vaccines used were DC-LLO_{91-99}, DC-$LLO_{296-304}$, DC-$LLO_{189-201}$, DC-$LLO_{189-200}$, DC-$LLO_{190-201}$, DC-$GAPDH_{1-15}$ and DC-$GAPDH_{1-22}$ (1×10^6 cells/mice). Mice were immunised into the peritoneal cavity (*i.p*) ($n = 5$) in the presence or absence of Advax (50 μg/ml) or left non-vaccinated (NV). Seven days after immunization, Balb/c and C57BL/6 mice were challenged *i.p* with 10^3 and 10^4 CFU of LM^{WT}/mice, respectively, and then bled before termination (Lauer et al., 2008). Sera were stored at −80 °C to measure cytokines by FACS analysis using the CBA kit that measures all Th1 cytokines of a sample at the same time (Becton Dickinson, Palo Alto, CA, USA). Data were analysed using the FlowJo software (Treestar, Ashland, OR). Samples were performed in triplicate and the results are the mean ± SD of two separate experiments. ANNOVA was used for statistics with the cytokine measurements. At termination spleens and livers were homogenized and CFUs counted in blood agar plates. To measure $CD4^+$ frequencies producing intracellular IFN-γ, spleen cells were cultured in 96-well plates (5×10^6 cells/ml) and stimulated with $GAPDH_{1-15}$ or $GAPDH_{1-22}$ peptides (5 μg/ml each peptide) for 5 h in the presence of brefeldin A as previously reported (Calderon-Gonzalez et al., 2014). Next, cells were surface labelled for CD4, fixed and permeabilized with cytofix/cytoperm kit before staining for intracellular IFN-γ (BD Biosciences). FACS data were analysed using FlowJo software (Treestar, Ashland, OR). After sample acquisition, data were gated for $CD4^+$ events, and the percentages of cells expressing IFN-γ determined according to the manufacturer's recommendations. Results were corrected according to the percentages of total $CD4^+$ cells. Samples were tested in triplicate and the results are the mean ± SD of two separate experiments.

2.8. Frequencies of $CD8^+$-LLO or GAPDH specific T cells

To confirm the frequency of LLO_{91-99}, $LLO_{296-304}$, $GAPDH_{1-15}$ or $GAPDH_{1-22}$ specific CD8 T cells producing IFN-γ, we used recombinant soluble dimeric mouse $H\text{-}2K^b$:Ig (for C57BL/6 mice) or $H\text{-}2L^d$:Ig (for Balb/c mice) fusion proteins following the manufacturer's instructions (DimerX I; BD Bioscience) and as previously described (Lauer et al., 2008; Calderon-Gonzalez et al., 2014).

2.9. ELISA for Listeria peptides

LLO_{91-99} or $GAPDH_{1-22}$ peptides were prepared at 50 μg/ml in coating buffer (50 nM of Na_2CO_3 at pH 9.7) and used to coat Nunc MaxiSorp plates overnight at 4 °C. Next, plates were blocked with 1% BSA in PBS at RT for 30 min and mice sera diluted 1/200 in PBS-0.5% BSA and incubated for 1 h at RT. Mice IgM was detected with a goat anti-mouse IgM conjugated with horseradish peroxidase (0.8 μg/ml) and enzymatic reactions developed with tetramethylbenzidine in citric/acetate buffer and H_2O_2. Reactions were stopped with 50 μl of H_2SO_4 (0.8 M) and absorbances measured at 450 nm in the ELISA reader. Results were expressed as absorbance units of triplicates ± SD.

2.10. Statistical analysis

For statistical analysis, Student's *t* test was applied. ANOVA analysis was applied to cytokine measurements. $P \leq 0.05$ was considered significant. GraphPad software was used for generation of graphs.

2.11. Ethics statement

This study was carried out in accordance with the Guide for the Care and Use of Laboratory Animals of the Spanish Ministry of Science, Research and Innovation. The Committee on the Ethics of Animal Experiments of the University of Cantabria approved the protocol (Permit Number: 2012/06) that follows the Spanish legislation (RD 1201/2005). All surgeries were performed under sodium pentobarbital anaesthesia, and all efforts were made to minimize suffering.

3. Results and discussion

3.1. Bioinformatics approach to classify Listeria epitopes

The objective of this study was to design a simple experimental approach that predicted the minimal epitope requirements to load and prepare DC vaccine formulations able to protect against listeriosis. We focussed on the *Listeria* antigens LLO and GAPDH as vaccine candidates since sera from patients recovering from listeriosis recognized various peptides from these antigens (Angelakopoulos et al., 2002; CAD and RCG unpublished results). Listeriosis is characterised by low humoral but robust T cell responses (Pamer, 2004). Previously T-cell epitopes for *Listeria* vaccine design have been identified by peptide elution from MHC molecules of *Listeria*-loaded macrophages (Geginat et al., 2001; Skoberne and Geginat, 2002). Since this approach is technically challenging, predominantly only identifies high affinity epitopes and is performed using macrophages which are less efficient at antigen presentation cells than DC, it may fail to identify many other relevant and protective *Listeria* T-cell epitopes. There is also no consensus of whether high, medium or low affinity epitopes may represent the best vaccine candidates. Bioinformatics approaches have been used in other infectious diseases to identify T-cell epitopes to include in vaccines with great success (Yu et al., 2002; Stephenson et al., 2015). Hence we used a bioinformatics approach to screen for potential T cell epitopes in LLO and GAPDH and followed this with a modified delayed-type-hypersensitivity (DTH) test to identify T-cell epitopes with potential to provide protection against human and veterinary listeriosis. As positive controls we used five known LLO epitopes previously identified by the elution method (Geginat et al., 2001). For T-cell epitope prediction we used IEDB, a bioinformatic prediction resource Consensus tool that combines predictions from artificial neural network (ANN), SMM and Comblib for GAPDH binding predictions (Nielsen et al., 2003; Peters and Sette, 2005; Sidney et al., 2008; Kim et al., 2012). IEDB analysis predicted that good MHC class I binders showed percentile ranks <10 and weak binders percentile ranks <100. Similarly, good MHC class II binders showed percentile thresholds <50, intermediate binders <500 and low binders <5000.

$GAPDH_{1-15}$ contained four epitopes predicted to be good binders for H-$2K^b$, H-$2K^d$ and H-$2L^d$ MHC-I molecules, and one predicted intermediate binding epitope for IA^b and low binder to IA^d (lower right image in Fig. 1A). $GAPDH_{1-22}$ contained six epitopes predicted to be good binders to H-$2K^d$ and H-$2L^d$, six epitopes predicted to be intermediate binders to IA^b and one epitope predicted to be a low binder to IA^d (GAPDH binding values in Fig. 1A). These data indicated that $GAPDH_{1-15}$ and $GAPDH_{1-22}$ epitopes were able to bind to different MHC-I and MHC-II molecules of Balb/c and C57BL/6 mice strains.

Analysis of LLO for epitopes indicated that LLO_{91-99} was predicted to be a strong binder to H-$2K^d$ (0.7 values) and also a weak binder to H-$2K^b$ MHC-I (67 values); $LLO_{296-304}$ peptide was predicted to be a strong binder to H-$2K^b$ (score 0.2), a weak binder to H-$2K^d$ (score 32) and an intermediate binder to H-$2L^d$ (score 12.5) and $LLO_{189-201}$ was predicted to be a strong binder to IA^b (score 51.3) and low binder to IA^d (score 5326). $LLO_{189-200}$ and $LLO_{190-201}$ peptides were not predicted to bind to IA^d (score > 10000) and to be weak binders to IA^b (scores 85 and 75, respectively) (Calderon-Gonzalez et al., 2015). All LLO epitope predictions were in agreement with the previously MHC-I and MHC-II eluted LLO epitopes (Geginat et al., 2001; Skoberne and Geginat, 2002). However, the bioinformatic analysis also predicted new MHC binding abilities for these LLO epitopes. Hence, the LLO_{91-99} epitope previously eluted from H-$2K^d$ was predicted to be a weak binder to H-$2K^b$, $LLO_{296-304}$ epitope eluted from H-$2K^b$ was predicted to be a weak binder to H-$2K^d$, $LLO_{189-201}$ and $LLO_{190-201}$ epitopes eluted from IA^b were predicted to be weak binders to IA^d, and $LLO_{189-200}$ epitope eluted from IA^d was predicted to be a weak binder to IA^b. Therefore, the bioinformatics analysis identified a higher number of potential binding epitopes than the elution methods. We next studied where the predicted LLO epitopes were situated within the recently reported LLO crystal structure (Köster et al., 2014) PBDI: 4CDB (left image, Fig. 1A). LLO showed 4 domains (D1, D2, D3 and D4) that contained several β-sheets and α-helices with D4 being the binding domain to the phagosomal membranes. Since no crystal structure from *Listeria* GAPDH was available, we used the Automated Comparative Protein Modelling Server SWISS-MODEL available at: (http://www.expasy-ch/swissmod/SWISS-MODEL.html) to produce a theoretical 3D model (right image, Fig. 1A). LLO epitopes that bind to MHC-I were tight or wide loops (pink and green LLO sequences, respectively, Fig. 1A), while epitopes that bind to MHC-II contained α-helices (purple LLO sequence, Fig. 1A). A similar pattern was observed for GAPDH, with $GAPDH_{1-22}$ and $GAPDH_{1-15}$ epitopes that bind to MHC-I containing tight loops and epitopes that bind to MHC-II molecules containing two α-helices. According to this rule, we predicted that $GAPDH_{1-22}$ and $GAPDH_{1-15}$ epitopes containing tight loops and two α-helices that are able to simultaneous bind to H-$2K^b$, H-$2K^d$, H-$2L^d$, IA^b and IA^d might be the best candidates for a T-cell based listeriosis vaccine. Next, the LLO_{91-99} epitope containing tight loops and $LLO_{296-304}$ epitope with wide loops that both bind to MHC-I molecules and the $LLO_{189-201}$ epitope containing two complete α-helices that bind to MHC-II molecules, were identified as good vaccine candidates as they were able to bind to MHC from both mice strains. $LLO_{189-200}$ and $LLO_{190-201}$ epitopes that contained one α-helix and bind to MHC-II molecules of one mice strain exclusively were classified using this algorithm as poor vaccine candidates.

3.2. Evaluation of the quality of DC vaccine formulations

Having identified candidate vaccine epitopes we next wished to exclude any negative effects of the relevant peptides on the viability of the proposed DC vaccine vectors. DC vectors need to remain viable to fully activate T cells in the draining lymph nodes, a process that takes at least 24 h. Therefore, we examined the effect of the relevant LLO and GAPDH peptides on DC cytotoxicity and activation after 24 h of culture, the time required for DC loading with peptides (Pion et al., 2010; Kono et al., 2012; Vacas-Cordoba et al., 2013; Calderon-Gonzalez et al., 2014). Cytotoxicity was examined with Trypan-blue staining and apoptosis

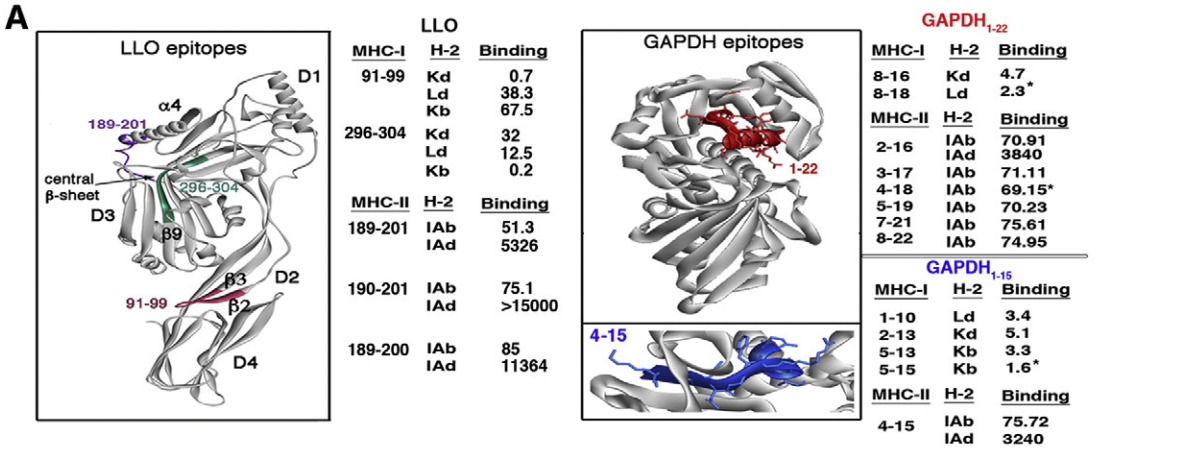

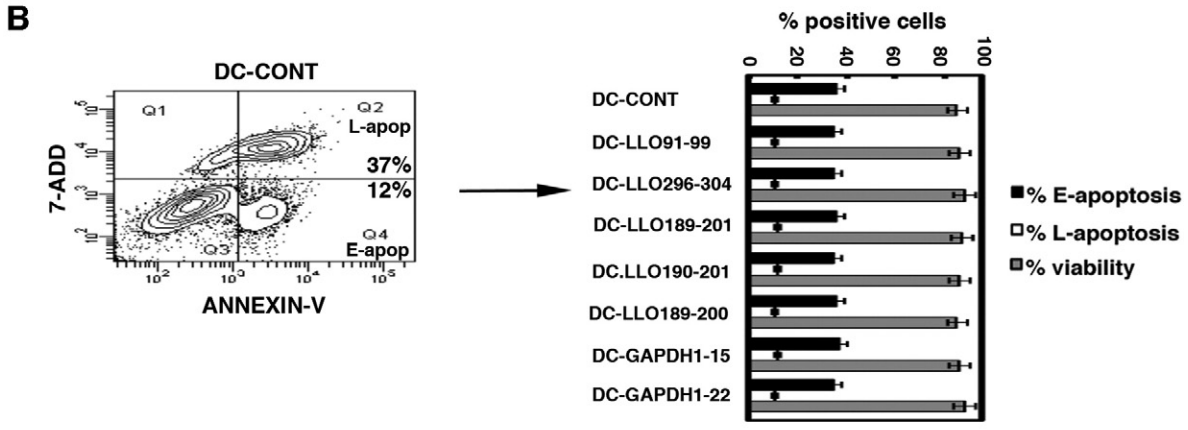

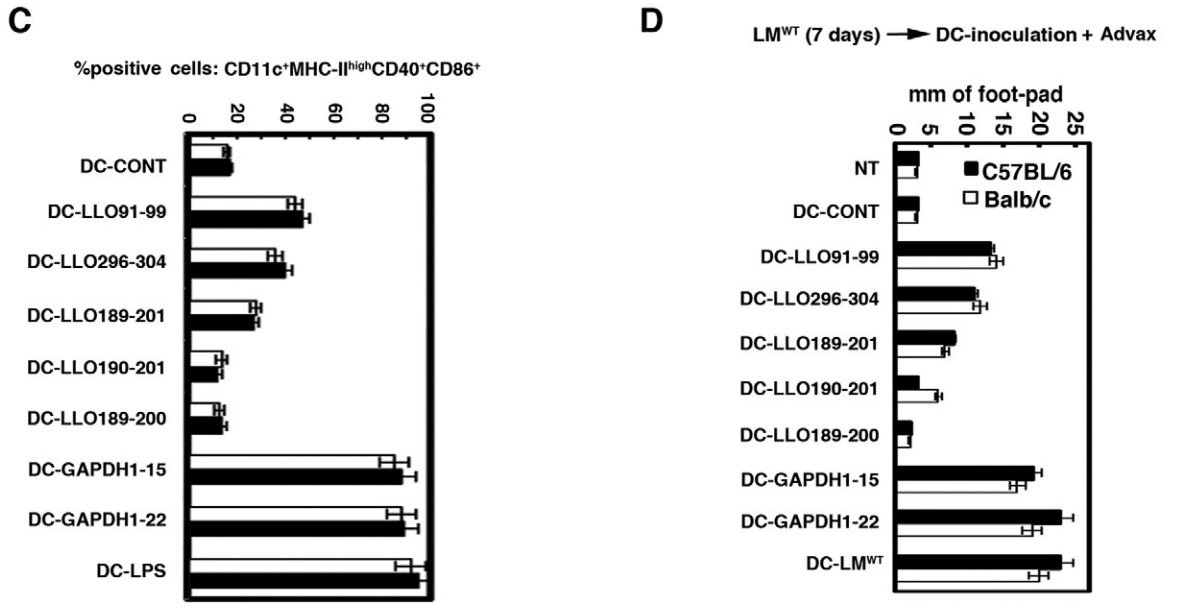

Fig. 1. Methodology to predict efficient vaccine epitopes for DC vaccine formulations. (A) diagram showing the bioinformatic strategy for epitope prediction including the 3D-structure of LLO based on the recently reported crystal structure (Köster et al., 2014) and the relevant MHC-I and MHC-II epitopes in Balb/c and C57BL/6 mice. The purple sequence corresponds to $LLO_{189–201}$ peptide that contains $LLO_{189–200}$ and $LLO_{190–201}$ MHC-II epitopes and the pink sequence corresponds to $LLO_{91–99}$ MHC-I epitope. The green sequence corresponds to the $LLO_{296–394}$ MHC-I epitope. On the right, the predicted 3D structure of GAPDH is shown with the $GAPDH_{1–22}$ peptide highlighted in red. The lower image shows an enlargement of amino acids 3–15 of $GAPDH_{1–15}$ epitope. The sequences included on the right correspond to MHC binding predictions performed with IEDB Consensus tool. (B) DCs were incubated with 50 μg/ml of peptides for 24 h and then stained with Trypan blue to assay cytotoxicity (grey bars) or incubated with 7-ADD and annexin-V to analyse apoptosis by FACS (black and white bars). An example of apoptosis read-out is shown in left panel. Cytotoxicity results are expressed as the number of cells ± SD and experiments were performed in triplicate. Apoptosis results are expressed as the mean of the percentages of early apoptotic (Q4 region), late apoptotic (Q2 region) or necrotic cells (Q1 region) ± SD ($P < 0.05$). (C) DC from Balb/c or C57BL/6 mice were differentiated *in vitro* with 30 ng/ml of GM-CSF for 5 days, detached and positively selected using anti-mouse CD11c-coated magnetic beads and MACS separation columns. $CD11c^+$ DC were loaded *ex vivo* with different peptides in the presence of 50 μg/ml of Advax: $LLO_{91–99}$, $LLO_{189–200}$, $LLO_{190–201}$, $LLO_{189–201}$, $LLO_{296–304}$, $GAPDH_{1–15}$ or $GAPDH_{1–22}$ peptides (50 μg/ml) for 24 h or left unloaded (DC-CONT). Cells were washed and analysed using a FACSCanto flow cytometer. The percentages of $CD11c^+MHC\text{-}II^{high}CD40^+CD86^+$ positive cells are shown. Results are expressed as the mean ± SD of triplicate samples ($P < 0.05$). (D) C57BL/6 (black bars) or Balb/c mice (white bars) were immunised *i.p* with 5×10^3 CFU of *Listeria*/mouse for 7 days and then left hind footpads were inoculated with 1×10^6 cells of different DC-LLO and DC-GAPDH vaccines or saline (NT) for 24 h in the presence of Advax (250 μg), while right hind footpads were not inoculated and served as controls. Footpad swelling was measured with a calliper and expressed as the differences in mm between left and right hind footpads. Results are expressed as the mean ± SD of three different experiments ($P < 0.05$).

with 7-ADD and annexin-V fluorescence (Fig. 1B and Table 1) using different concentrations of LLO_{91-99}, $LLO_{189-201}$, $LLO_{189-200}$, $LLO_{190-201}$, $LLO_{296-304}$, $GAPDH_{1-15}$ or $GAPDH_{1-22}$ peptides (0–500 μg/ml). None of the LLO or GAPDH peptides at doses of 50 μg/ml and below caused DC cytotoxicity, early (E-apo of Q4 region or E-apoptosis in black bars of Fig. 1B) or late apoptosis (L-apop of Q2 region or L-apoptosis in white bars of Fig. 1B). As the highest concentrations of peptides (500 μg/ml) were associated with slightly lower DC viability (Table 1), we selected 50 μg/ml as the on-going loading concentration for our DC vaccines.

An important issue for DC vaccines is their activation state, as this improves the quality of the resulting T-cell responses. Activated DCs show a characteristic $CD11c^+MHC\text{-}II^+CD40^+CD86^+$ phenotype that corresponds with higher vaccine efficiency (Pion et al., 2010; Kono et al., 2012; Vacas-Cordoba et al., 2013). Peptides by themselves generally do not activate DC, although longer peptides may sometimes do so (Calderon-Gonzalez et al., 2014). Since LLO and GAPDH peptides differ significantly in their length, we standardised the experiment by mixing the peptides with 50 μg/ml of Advax adjuvant prior to DC loading for 24 h. Advax was included, as it has been previously shown to modulate DC activity and potently enhance $CD4^+$ and $CD8^+$ T cell responses to *Listeria* antigens (Rodriguez-Del Rio et al., 2015). We also included LPS (10 ng/ml) as a classical DC activator (DC-LPS) (Kono et al., 2012; Calderon-Gonzalez et al., 2014) as well as untreated control DC (DC-CONT). LPS induced the highest frequency of $CD11c^+MHC\text{-}II^{high}CD40^+CD86^+$ DC ($CD11c^+$ DC) followed by $GAPDH_{1-22}$ and $GAPDH_{1-15}$ peptides. LLO_{91-99} induced intermediate numbers of $CD11c^+$ DC. $LLO_{296-304}$ and $LLO_{189-201}$ peptides also induced significant numbers of $CD11c^+$ DC while $LLO_{189-200}$ and $LLO_{190-201}$ induced no $CD11c^+$ DC at all (Fig. 1C).

We applied these results to the bioinformatics predictions to identify whether there were any epitope characteristics, which predicted the highest DC activation in both mice strains. Notably, the $GAPDH_{1-15}$ epitope that induced a high DC activation (Fig. 1C) had four MHC-I binding sequences in tight loops and one MHC-II binding sequence containing two α-helices (Fig. 1A). Intermediate DC activation occurred with the LLO_{91-99} epitope (DC-LLO_{91-99} bars in Fig. 1C) that corresponded with a tight loop (pink LLO loop in Fig. 1A) that binds to MHC-I molecules in both mice strains. Lower DC activation was observed with $LLO_{296-304}$ epitopes (DC-$LLO_{296-304}$ bars in Fig. 1C), which corresponded with a wide loop that binds to MHC-I molecules in both mice strains (green LLO epitopes in Fig. 1A). Very low DC activation was observed only with $LLO_{189-201}$ epitope (DC-$LLO_{189-201}$ bars in Fig. 1C) that corresponded with two complete α-helices that bind to MHC-II molecules in both mice strains (purple LLO epitopes in Fig. 1A). No DC activation was observed with $LLO_{189-200}$ or $LLO_{190-201}$ epitopes (Fig. 1C) that corresponded with one α-helix that binds exclusively to MHC-II of only one mice strain. This analysis suggests that epitopes that bind MHC-I are more likely to induce DC activation than MHC-II binders.

Table 1
Lack of cytoxicity induction of LLO and GAPDH peptides.

Reagent	DC viability[a]
LLO_{91-99} (μg/ml)	
500	$1.69 \pm 0.132 \times 10^6$
50	$1.79 \pm 0.120 \times 10^6$
5	$1.78 \pm 0.113 \times 10^6$
0.5	$1.79 \pm 0.128 \times 10^6$
$LLO_{189-201}$ (μg/ml)	
500	$1.69 \pm 0.132 \times 10^6$
50	$1.77 \pm 0.120 \times 10^6$
5	$1.78 \pm 0.113 \times 10^6$
0.5	$1.79 \pm 0.128 \times 10^6$
$LLO_{190-201}$ (μg/ml)	
500	$1.69 \pm 0.132 \times 10^6$
50	$1.76 \pm 0.120 \times 10^6$
5	$1.78 \pm 0.113 \times 10^6$
0.5	$1.79 \pm 0.128 \times 10^6$
$LLO_{190-201}$ (μg/ml)	
500	$1.67 \pm 0.132 \times 10^6$
50	$1.78 \pm 0.120 \times 10^6$
5	$1.78 \pm 0.113 \times 10^6$
0.5	$1.79 \pm 0.128 \times 10^6$
$LLO_{296-304}$ (μg/ml)	
500	$1.61 \pm 0.132 \times 10^6$
50	$1.77 \pm 0.120 \times 10^6$
5	$1.78 \pm 0.113 \times 10^6$
0.5	$1.79 \pm 0.128 \times 10^6$
$GAPDH_{1-15}$ (μg/ml)	
500	$1.73 \pm 0.132 \times 10^6$
50	$1.78 \pm 0.120 \times 10^6$
5	$1.78 \pm 0.113 \times 10^6$
0.5	$1.79 \pm 0.128 \times 10^6$
$GAPDH_{1-22}$ (μg/ml)	
500	$1.69 \pm 0.132 \times 10^6$
50	$1.78 \pm 0.120 \times 10^6$
5	$1.78 \pm 0.113 \times 10^6$
0.5	$1.79 \pm 0.128 \times 10^6$

[a] *In vitro* cytoxicity assayed using DC incubated with different doses of peptides (0–500 μg/ml) for 24 h and then stained with Trypan blue. Results are expressed as the number of viable cells ± SD and experiments were performed in triplicates ($P < 0.05$).

3.3. Quantification of T-cell responses elicited by DC-vaccine formulations

Next we sought to develop an assay to predict the DC epitopes that elicited the highest T cell responses, *in vivo*. For this purpose, we adapted a classical delayed-type-hypersensitivity (DTH) test (Mohamed et al., 2012), where DC vaccines loaded with LLO or GAPDH peptides plus Advax adjuvant (50 μg/ml) were inoculated into the foot pads of previously *Listeria*-challenged mice and the DTH response measured as the degree of footpad swelling 24 h post-inoculation (Fig. 1D). We included a positive control of DTH response, DC infected *in vitro* with wild type LM (DC-LM^{WT}) that induced a high degree of footpad swelling as previously reported (Calderon-Gonzalez et al., 2015). In both mice strains, DC-$GAPDH_{1-15}$ and DC-$GAPDH_{1-22}$ vaccines generated the highest DTH responses, similar to the positive control DC-LM^{WT}, followed by DC-LLO_{91-99}, then DC-$LLO_{296-304}$ and lastly DC-$LLO_{189-201}$. DC-$LLO_{190-201}$ induced a low DTH response only in susceptible Balb/c mice and DC-$LLO_{189-200}$ induced no response in either strain (Fig. 1D). These results indicated that the size of the DTH responses elicited by the DC epitope vaccines formulated with Advax adjuvant, correlated well with the ability of the peptides to induce DC activation and with the initial bioinformatic predictions (Fig. 1B–C). The removal of Advax adjuvant from the DC vaccine formulations reduced all DTH results ~5-fold but the Advax adjuvant did not modify the controls (data not shown), confirming that its action was *via* enhancement of antigen-specific T-cell responses. This is consistent with enhancement of antigen-specific T-cell responses observed with Advax adjuvant in other contexts such as when combined with influenza, hepatitis B or SARS coronavirus vaccines (Honda-Okubo et al., 2012, 2015; Saade et al., 2013).

Next, we tested whether the strong DTH results for specific DC vaccines correlated with a Th1 cytokine response, as reflected in the supernatants of DC loaded with the different LLO and GAPDH peptides in the presence of Advax adjuvant as in Fig. 1A. We observed that for both mouse strains, DC-$GAPDH_{1-22}$, DC-$GAPDH_{1-15}$ and DC-LLO_{91-99} vaccines induced the highest TNF-α levels followed by DC-$LLO_{296-304}$. DC-$LLO_{189-201}$, DC-$LLO_{190-201}$ and DC-$LLO_{189-200}$ vaccines induced no TNF-α (Table 2). Only DC-$GAPDH_{1-22}$ and DC-$GAPDH_{1-15}$ induced significant levels of IL-12 in both mice strains, with IL-12 having been shown to correlate with protective vaccine responses against listeriosis (Kono et al., 2012 and Calderon-Gonzalez et al., 2014). DC-LLO_{91-99} vaccines produced low but significant levels of IL-12 in both mice strains

Table 2
Th1 cytokines production by DC vaccines loaded with peptides in the presence of Advax.

Epitope[a]	Th1-cytokines (pg/ml)[b]		
	Cytokines	Balb/c	C57BL/6
LLO_{91-99}	TNF-α	1495 ± 102	1475 ± 118
	IL-12	4.5 ± 0.1*	0.45 ± 0.05
$LLO_{296-304}$	TNF-α	315 ± 0.9	310 ± 0.9
	IL-12	0 ± 0	0 ± 0
$LLO_{190-201}$	TNF-α	15 ± 0.7	10 ± 0.8
	IL-12	0.11 ± 0	0.12 ± 0.04
$LLO_{189-200}$	TNF-α	10 ± 0.8	11 ± 0.7
	IL-12	0 ± 0	0 ± 0
$LLO_{189-201}$	TNF-α	25 ± 0.9	20 ± 0.9
	IL-12	0 ± 0	0 ± 0
$GAPDH_{1-22}$	TNF-α	1635 ± 100	1721 ± 113
	IL-12	25 ± 0.8*	24 ± 0.8*
$GAPDH_{1-15}$	TNF-α	1515 ± 120	1510 ± 138
	IL-12	24 ± 0.8*	22 ± 0.9*

Asterisks show the IL-12 significant levels.
[a] Levels of pro-inflammatory TNF-α and IL-12 cytokines were analysed in sera of different DC vaccinated Balb/c or C57BL/6 mice in the presence of Advax adjuvant (50 μg/ml) by CBA. Results are expressed as cytokine concentration (pg/ml of mean ± SD, $P < 0.05$).

whereas DC-$LLO_{296-304}$, DC-$LLO_{189-201}$, DC-$LLO_{190-201}$ and DC-$LLO_{189-200}$ induced no detectable IL-12 levels (Table 2). Thus, only the DC epitopes originally predicted by bioinformatic analysis to be the best CD8 T-cell epitopes and which produced the highest DTH responses *in vivo* were associated with significant IL-12 production by DC.

3.4. Validation of proposed methods of epitope prediction for listeriosis vaccines

Next, to verify the above predictions, susceptible Balb/c and resistant C57BL/6 mice were immunized with DC-LLO_{91-99}, DC-$LLO_{296-304}$, DC-$LLO_{189-200}$, DC-$LLO_{190-201}$, DC-$LLO_{189-201}$, DC-$GAPDH_{1-15}$, or DC-$GAPDH_{1-22}$ together with Advax (50 μg/ml) or were left non-vaccinated (NV). Mice were immunized *i.p* with a single dose of vaccine and 7 days later were administered a *Listeria* challenge (see Methods section for procedures). Five days post-challenge, all mice were bled, sacrificed and spleens recovered to count *Listeria* CFU and analyse immune cell populations (Fig. 2A and Table 3). DC-$GAPDH_{1-15}$ and DC-$GAPDH_{1-22}$ provided the greatest protection in both Balb/c and C57BL/6 mice (~97 and 99%, respectively) (Fig. 2A). DC-LLO_{91-99} also conferred significant protection in both Balb/c and C57BL/6 mice (90 and 93%, respectively). DC-$LLO_{296-304}$ vaccine conferred strong protection in C57BL/6 mice (~90%) (Fig. 2A) but only intermediate levels of protection in Balb/c mice (~60%) (white bars in Fig. 2A). DC-$LLO_{189-200}$, DC-$LLO_{190-201}$, and DC-$LLO_{189-201}$ vaccines conferred no significant protection in either strain (2 and 5%, respectively). Vaccination efficiency was associated with normal spleen size (images of DC-$GAPDH_{1-15}$ vaccine recipients shown in Fig. 2A) compared with enlarged spleens (images of NV mice in Fig. 2A) and granulomatous livers of non-vaccinated mice (data not shown). We also evaluated several immunological parameters induced by the most protective DC vaccines. DC-$GAPDH_{1-15}$ and DC-$GAPDH_{1-22}$ vaccines were found to induce the highest frequencies of IFN-γ-producing $CD8^+$ T cells in both C57BL/6 and Balb/c mice (4.0–4.2%, respectively) followed by DC-LLO_{91-99} vaccine with 3.0% frequency as assessed by FACS using H2-K^b:Ig-peptide dimers or 2.16% frequency using H2-L^d:Ig-peptide dimers (right plot in Fig. 2B). DC-$LLO_{296-304}$ vaccine induced very low 0.87% $CD8^+$ T cell frequencies in C57BL/6 mice and undetectable frequencies in Balb/c mice (DC-$LLO_{296-304}$ bars in Fig. 2B). Only DC-$GAPDH_{1-15}$ and DC-$GAPDH_{1-22}$ vaccines induced detectable numbers of IFN-γ producing peptide-specific $CD4^+$ T cells (1.05 and 1.76%, respectively) (Fig. 2B show C57BL/6 data, values in Balb/c were 1.05 and 1.76%). In summary, our results with DC-GAPDH vaccines confirmed that $CD8^+$ T cell responses were more relevant than $CD4^+$ T cell responses for *Listeria* protection. $GAPDH_{1-15}$ and $GAPDH_{1-22}$ peptides presented high numbers of MHC-I binding epitopes in listeriosis resistant and sensible mice, explaining DC-GAPDH vaccines induced similar $CD8^+$ T cell responses and Th1-cytokines in both mice strains.

Antibody production and B cell responses seemed to play no role in listeriosis (Pamer, 2004). However, antibodies against LLO seemed to participate in neutralization of *Listeria* growth (Edelson and Unanue, 2001). Here, we confirmed no variation in B cell numbers among non-vaccinated (NV), vaccinated mice (DC vaccines) or non-infected control mice (control) with similar percentages of $CD19^+$ positive cells (Spleen markers rows in Table 3). Nevertheless, DC-$GAPDH_{1-22}$ (DC-$GAPDH_{1-22}$ rows in Table 3) or DC-$GAPDH_{1-15}$ vaccines (data not shown) produced high levels of anti-$GAPDH_{1-22}$ IgM antibodies compared to non-vaccinated mice (NV) that correlated with an increase in the percentages of $CD4^+$ T cells. DC-LLO_{91-99} vaccinated mice produced no significant levels of anti-LLO_{91-99} IgM antibodies compared to NV and presented low percentages of $CD4^+$ T cells (DC-LLO_{91-99} rows in Table 3). These data strongly suggested that vaccines conferring the highest protection in listeriosis induced prominent antigen-specific T cell responses and promoted also antigen-specific B cell responses, suggesting a collaborative role of B and T cell responses in listeriosis protection (Edelson and Unanue, 2001; Alvarez-Dominguez et al., 2008; Calderon-Gonzalez et al., 2014, 2015).

Finally, vaccination with DC-$GAPDH_{1-15}$, DC-$GAPDH_{1-22}$ or DC-LLO_{91-99} vaccine induced high levels of MCP-1, TNF-α and IFN-γ in both mice strains whereas DC-$LLO_{296-304}$ vaccine induced only intermediate levels of TNF-α in C57BL/6 mice (DC-$LLO_{296-304}$ bars in Fig. 2C). Only DC-$GAPDH_{1-15}$ and DC-$GAPDH_{1-22}$ vaccines induced high IL-12 levels, post-challenge, in both mice strains (right plot in Fig. 2C). DC-LLO_{91-99} vaccine induced low but significant levels of IL12 in both mice strains (Kono et al., 2012; Calderon-Gonzalez et al., 2014). Thus the *Listeria* T-cell epitope prediction algorithm described in the methods was validated *in vivo* and shown to predict vaccine effectiveness after *Listeria* vaccination of low and high susceptibility mice. Advax adjuvant was confirmed to be important to induction of a potent *Listeria* antigen specific T-cell response, consistent with its ability to enhance vaccine protection in other models including influenza, where it similarly enhanced $CD4^+$ and $CD8^+$ T-cell responses and Th1 cytokine production (Honda-Okubo et al., 2012). The present results confirm that Advax adjuvant has the ability to induce MHC I cross-presentation of *Listeria* antigens thereby resulting in activation of *Listeria*-specific CD8 T cells, although the mechanism by which it might induce cross-presentation is currently unknown. One possibility currently under investigation is that Advax induces cross-presentation *via* activation of $CD4^+$ T helper cells that signal to upregulate cross-presentation pathways in antigen presenting cells. When considering design of *Listeria* vaccines, a major advantage of Advax over other potential T-cell adjuvants is its lack of toxicity as evidenced by data from preclinical studies (Lobgis et al., 2010; Cristillo et al., 2011; Eckersley et al., 2011; Layton et al., 2011; Larena et al., 2013; Petrovsky et al., 2013; Saade et al., 2013; Bielefeldt-Ohmann et al., 2014; Feinen et al., 2014; Honda-Okubo et al., 2014, 2015) as well as human clinical trials (Gordon et al., 2012, 2014).

4. Conclusions

New methods of T-cell epitope screening would greatly assist design of DC vaccine formulations, including for protection against listeriosis. Here we have developed a method for DC vaccine design that combines bioinformatic prediction of MHC binding epitopes with 3D structural predictions and DC functional assays utilising Advax, a potent T-cell adjuvant, to amplify the signal. Using these methodologies, we successfully predicted *Listeria* epitopes that when incorporated in DC vaccines and administered to either Balb/c or C57BL/6 mice were able to confer protection against *Listeria* challenge. Peptides binding at least four MHC-I

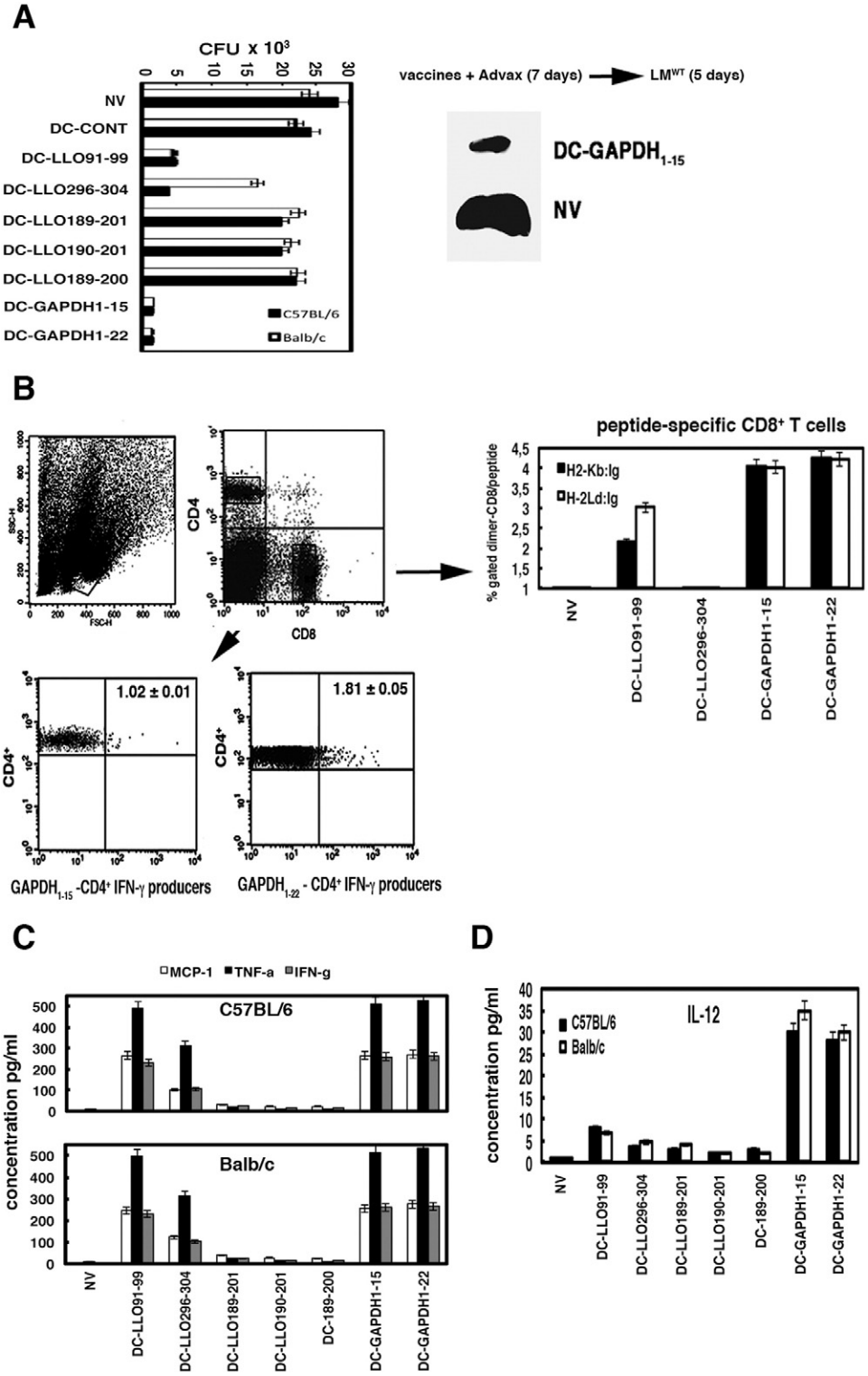

Fig. 2. Experimental validation of epitope predictions with vaccination assays. DC vaccines were tested for their immunogenicity and ability to protect against listeriosis. (A) C57BL/6 (black bars) or Balb/c (white bars) mice were vaccinated *i.p* with different DC vaccine vectors ($1 \times 10_6$ cells). DC-CONT, DC-GAPDH$_{1-15}$, DC-GAPDH$_{1-22}$, DC-LLO$_{91-99}$, DC-LLO$_{296-304}$, DC-LLO$_{189-200}$, DC-LLO$_{189-201}$ or DC-LLO$_{190-201}$ in the presence of Advax (50 μg/ml) or left not vaccinated (NV) (n = 5 mice/group) and 7 days later were challenged *i.p* with 10_3 CFU LM (for Balb/c mice) or 10_4 CFU LM (for C57BL/6 mice). Results of spleen homogenates are expressed as CFU (mean ± SD) and obtained from triplicate samples of three independent experiments ($P < 0.01$). Images correspond to spleens of non-vaccinated mice (NV) showing splenomegaly *versus* DC-GAPDH$_{1-15}$ vaccinated C57BL/6 mice. (B) C57BL/6 or Balb/c mice were vaccinated and then challenged with LM as in A and examined for specific GAPDH T-cell responses by intracellular cytokine staining (lower plots). Homogenates were stimulated 5 h with GAPDH$_{1-15}$ or GAPDH$_{1-22}$ peptides then intracellular cytokine staining performed. Histograms show the frequency of GAPDH$_{1-15}$ (left lower plot) and GAPDH$_{1-22}$-specific CD4+ T cells (right lower plot) and IFN-γ producers in C57BL/6 spleen homogenates. Experiments were performed in triplicate and results are expressed as mean ± SD ($P < 0.05$). To measure the frequencies of CD8+ GAPDH-specific immune responses (right plots), splenocytes from vaccinated mice were incubated with recombinant dimeric H-2K$_b$:Ig (black bars) or H-2L$_d$:Ig (white bars) fusion proteins loaded with LLO$_{91-99}$, LLO$_{296-304}$, GAPDH$_{1-15}$ or GAPDH$_{1-22}$ peptides, respectively. The staining cocktail contained the dimeric fusion protein loaded with the peptides, CD8 and IFN-γ antibodies. CD8+ cells were gated for anti-IFN-γ staining (% Gated dimer-CD8) to calculate the frequencies of CD8+-GAPDH$_{1-15}$ or CD8+-GAPDH$_{1-22}$ restricted cells and IFN-γ producers. Results were expressed as the mean ± SD of triplicates ($P < 0.05$). (C) Levels of pro-inflammatory cytokines MCP-1, TNF-α or IFN-γ were analysed in mouse sera from DC-vaccinated and LM challenged mice as in A using the CBA kit (BD Biosciences) by flow cytometry (see Material and Methods). Upper plot correspond to cytokine measurements of C57BL/6 mice and lower plot to Balb/c mice. Results expressed as cytokine concentration (pg/ml) of mean ± SD, $P < 0.05$. (D), IL-12 levels of sera from A measured with the CBA kit and expressed as cytokine concentration (pg/ml) of mean ± SD, $P < 0.05$.

Table 3
B cell responses elicited by DC-vaccines in the presence of Advax.

Vaccine[a]	Anti-peptide IgM antibodies[b]	
	LLO_{91-99}	$GAPDH_{1-22}$
Control	0.156 ± 0.05	0.163 ± 0.04
NV	0.517 ± 0.02	1.021 ± 0.02
DC-$GAPDH_{1-22}$	0.712 ± 0.02	2.011 ± 0.05
DC-LLO_{91-99}	0.583 ± 0.03	1.276 ± 0.02

Vaccine[a]	Spleen markers[c]			
	$CD19^+$	$CD4^+$	$CD8^+$	$CD11c^+$-$CD86^+$
Control	19 ± 0.5	7 ± 0.3	8 ± 0.2	0.5 ± 0.02
NV	15 ± 0.5	18 ± 0.6	17 ± 0.5	26 ± 0.8
DC-$GAPDH_{1-22}$	15 ± 0.3	26 ± 0.4	28 ± 0.5	70 ± 0.7
DC-LLO_{91-99}	15 ± 0.2	7 ± 0.2	27 ± 0.3	70 ± 0.6

[a] C57BL/6 (Table) or Balb/c (data not shown) mice were vaccinated in the presence of Advax (50 μg/ml) with DC-$GAPDH_{1-22}$ or DC-LLO_{91-99} vaccines or non-vaccinated (NV). 7 days post-vaccination, vaccinated and NV mice were infected with 5×10^3 CFU of LM^{WT} for 5 days. Control mice were non-vaccinated and non-infected. Next, mice were sacrificed and sera collected and stored at −80 °C. Spleens were homogenized for further analysis.

[b] Sera from vaccinated, non-vaccinated or control mice were thawed and examined peptide-ELISA as described in Methods section. Reactions were developed with goat anti-mouse IgM and absorbances analysed at 450 nm. Results are the mean of triplicates ± SD.

[c] Cell surface markers were examined in spleens of vaccinated, non-vaccinated or control mice after incubation with different antibodies conjugated with fluorochromes and analyse by FACS. Results corresponded to the mean of the percentages of positive cells ± SD.

molecules with high affinity due to tight loops and also containing a weaker MHC-II binding epitope containing two α-helices, elicited the highest DC activation, the strongest DTH immune responses and the highest production of IL-12. These properties conferred the greatest protection in mouse strains at either high or low susceptibility to listeriosis. The $GAPDH_{1-15}$ epitope possessed these minimal requirements and proved to have similar protective efficacy to the longer $GAPDH_{1-22}$ epitope. This methodology might help to design new human and veterinary vaccines against listeriosis, an area of need given the increasing incidence of this disease in European countries (Peña-Sagredo et al., 2008; Valero and Rafart, 2014; Pérez-Trallero et al., 2014). The methodology used in this study to predict the best T-cell epitopes for vaccine design, might be useful in design of DC vaccines against other infectious diseases, and notably the protective $GAPDH_{1-15}$ epitope showed 98% homology with *S. pneumonia* and *Streptococcus pyogenes* (Alvarez-Dominguez et al., 2008).

Disclosures

NP is a Director of Vaxine Pty Ltd, which holds rights over Advax™ adjuvant.

Acknowledgements

This study was supported in part by MINECO grants, SAF2009-08695 and SAF2012-34203 and Institutional grants API2012/03/SAF2009-08695 and AIP2014/SAF2012-34203 (to C. A-D). We acknowledge the laboratory technical assistance of L. V-R, the peptide synthesis by F. Roncal (CNB, CSIC, Madrid), the IDIVAL institutional assistance of C. Santacruz-Llata with FACS analysis and the *Listeria* strains provided by D. A. Portnoy (UCLA. USA). Development of Advax™ adjuvant was supported by contract HHSN272200800039C to Vaxine from the National Institute of Allergy and Infectious Diseases, National Institutes of Health. This paper's contents are solely the responsibility of the authors and do not necessarily represent the official views of the National Institutes of Health.

References

Alvarez-Dominguez, C., Madrazo-Toca, F., Fernandez-Prieto, L., Vandeckerhove, J., Pareja, E., Tobes, R., Gomez-Lopez, M.T., Del Cerro-Vadillo, E., Fresno-Escudero, M., Leyva-Cobián, F., Carrasco-Marin, E., 2008. Characterization of a *Listeria monocytogenes* protein interfering with Rab5a. Traffic 9, 325.

Angelakopoulos, H., Loock, K., Sisul, D.M., Jensen, E.R., Miller, J.F., Hohmann, E.L., 2002. Safety and shedding of an attenuated strain of *Listeria monocytogenes* with a deletion of actA/plcB in adult volunteers: a dose escalation study of oral inoculation. Infect. Immun. 70 (7), 3592.

Bielefeldt-Ohmann, H., Prow, N.A., Wang, W., Tan, C.S., Coyle, M., Douma, A., Hobson-Peters, J., Kidd, L., Hall, R.A., Petrovsky, N., 2014. Safety and immunogenicity of a delta inulin-adjuvanted inactivated Japanese encephalitis virus vaccine in pregnant mares and foals. Vet. Res. 45, 130. http://dx.doi.org/10.1186/s13567-014-0130-7.

Calderon-Gonzalez, R., Frande-Cabanes, E., Bronchalo-Vicente, L., Lecea-Cuello, M.J., Pareja, E., Bosch-Martinez, A., Fanarraga, M.L., Yañez-Diaz, S., Carrasco-Marin, E., Alvarez-Dominguez, C., 2014. Cellular vaccines in listeriosis: role of the *Listeria* antigen GAPDH. Front. Cell. Infect. Microbiol. 4 (22), 1–11. http://dx.doi.org/10.3389/fcimb.2014.00022. eCollection 2014.

Calderon-Gonzalez, R., Frande-Cabanes, E., Tobes, R., Pareja, E., Alaez-Alvarez, L., Alvarez-Dominguez, C., 2015. A dendritic cell targetted vaccine loaded with a glyceraldehyde-3-phosphate-dehydrogenase peptide proposed for individuals at high risk of listeriosis. J. Vaccines Vaccin. 6, 266. http://dx.doi.org/10.4172/2157-7560.1000266.

Cohen, N., Margalit, R., Pevsner-Fischer, M., Yona, S., Jung, S., Eisenbach, L., Cohen, I.R., 2012. Mouse dendritic cells pulsed with capsular polysaccharide induce resistance to lethal pneumococcal challenge: roles of T cells and B cells. PLoS One 7 (6), e39193.

Cooper, P.D., Petrovsky, N., 2011. Delta inulin: a novel, immunologically active, stable packing structure comprising β-D-[2- > 1] poly(fructo-furanosyl) α-D-glucose polymers. Glycobiology 21 (5), 595. http://dx.doi.org/10.1093/glycob/cwq201.

Cooper, P.D., Barclay, T.G., Ginic-Markovic, M., Petrovsky, N., 2013. The polysaccharide inulin is characterized by an extensive series of periodic isoforms with varying biological actions. Glycobiology 23 (10), 1164.

Cooper, P.D., Barclay, T.G., Ginic-Markovic, M., Gerson, A.R., Petrovsky, N., 2014. Inulin isoforms differ by repeated additions of one crystal unit cell. Carbohydr. Polym. 103, 392. http://dx.doi.org/10.1016/j.carbpol.2013.12.066.

Cooper, P.D., Rajapaksha, K.H., Barclay, T.G., Ginic-Markovic, M., Gerson, A.R., Petrovsky, N., 2015. Inulin cristal initiation via a glucose-fructose cross-link of adjacent polymer chains: atomic force microscopy and static molecular modelling. Carbohydr. Polym. 117, 964. http://dx.doi.org/10.1016/j.carbpol.2014.10.022.

Cristillo, A.D., Ferrari, M.G., Hudacik, L., Lewis, B., Galmin, L., Bowen, B., Thompson, D., Petrovsky, N., Markham, P., Pal, R., 2011. Induction of mucosal and systemic antibody and T-cell responses following prime-boost immunization with novel adjuvanted human immunodeficiency virus-1-vaccine formulations. J. Gen. Virol. 92 (Pt 1), 128.

Eckersley, A.M., Petrovsky, N., Kinne, J., Wernery, R., Wernery, U., 2011. Improving the dromedary antibody response: the hunt for the ideal camel adjuvant. J. Camel Pract. Res. 18 (1), p35.

Edelson, B., Unanue, E.R., 2001. Intracellular antibody neutralizes *Listeria* growth. Immunity 14 (5), 503.

Feinen, B., Petrovsky, N., Verma, A., Merkel, T.J., 2014. Advax-adjuvanted recombinant protective antigen provides protection against inhalational anthrax that is further enhanced by addition of murabutide adjuvant. Clin. Vaccine Immunol. 21 (4), 580. http://dx.doi.org/10.1128/CVI.00019-14.

Fromen, C.A., Robbins, G.R., Shen, T.W., Kai, M.P., Ting, J.P., DeSimone, J.M., 2015. Controlled analysis of nanoparticle charge on mucosal and systemic antibody responses following pulmonary immunization. Proc. Natl. Acad. Sci. U. S. A. 112 (2), 488.

Geginat, G., Schenk, S., Skoberne, M., Goebel, W., Hof, H., 2001. A novel approach of direct ex vivo epitope mapping identifies dominant and subdominant CD4 and CD8 T cell epitopes from *Listeria monocytogenes*. J. Immunol. 166, 1877.

Gordon, D.L., Sajkov, D., Woodman, R.J., Honda-Okubo, Y., Cox, M.J., Heinzel, S., Petrovsky, N., 2012. Randomized clinical trial of immunogenicity and safety of a recombinant H1N1/2009 pandemic influenza vaccine containing Advax™ polysaccharide adjuvant. Vaccine 30, 5047.

Gordon, D., Kelley, P., Heinzel, S., Cooper, P., Petrovsky, N., 2014. Immunogenicity and safety of Advax™, a novel polysaccharide adjuvant based on delta inulin, when formulated with hepatitis B surface antigen: a randomized controlled phase 1 study. Vaccine http://dx.doi.org/10.1016/j.vaccine.2014.09.034 (Sep 26. pii: S0264-410X(14)01293-6).

Honda-Okubo, Y., Saade, F., Petrovsky, N., 2012. Advax™, a polysaccharide adjuvant derived from delta inulin, provides improved influenza vaccine protection through broad-based enhancement of adaptive immune responses. Vaccine 30 (36), 5373–5381. http://dx.doi.org/10.1016/j.vaccine.2012.06.021.

Honda-Okubo, Y., Kolpe, A., Li, L., Petrovsky, N., 2014. A single immunization with inactivated H1N1 influenza vaccine formulated with delta inulin adjuvant (Advax™) overcomes pregnancy-associated immune suppression and enhances passive neonatal protection. Vaccine 32 (36), 4651 (2014 Aug 6).

Honda-Okubo, Y., Barnard, D., Ong, C.H., Peng, B.H., Tseng, C.T., Petrovsky, N., 2015. Severe acute respiratory syndrome-associated coronavirus vaccines formulated with delta inulin adjuvants provide enhanced protection while ameliorating lung eosinophilic immunopathology. J. Virol. 89 (6), 2995. http://dx.doi.org/10.1128/JVI.02980-14.

Kawasaki, N., Rillahan, C.D., Cheng, T.Y., Van Rhijn, I., Macauley, M.S., Moody, D.B., Paulson, J.C., 2014. Targeted delivery of mycobacterial antigens to human dendritic cells via Siglec-7 induces robust T cell activation. J. Immunol. 193 (4), 1560.

Kim, Y., Ponomarenko, J., Zhu, Z., Tamang, D., Wang, P., Greenbaum, J., Lundegaard, C., Sette, A., Lund, O., Bourne, P.E., Nielsen, M., Peters, B., 2012. Immune epitope database analysis resource. Nucleic Acids Res. 40 (Web Server issue), W525. http://dx.doi.org/10.1093/nar/gks438 (Epub 2012 May 18).

Kono, M., Nakamura, Y., Suda, T., Uchijima, M., Tsujimura, K., Nagata, T., Giermasz, A.S., Kalinski, P., Nakamura, H., Chida, K., 2012. Enhancement of protective immunity against intracellular bacteria using type-1 polarized dendritic cell (DC) vaccine. Vaccine 30, 2633.

Köster, S., van Pee, K., Hudel, M., Leustik, M., Rhinow, D., Kühlbrandt, W., Chakraborty, T., Yildiz, Ö., 2014. Crystal structure of listeriolysin O reveals molecular details of oligomerization and pore formation. Nat. Commun. 5, 3690. http://dx.doi.org/10.1038/ncomms4690.

Larena, M., Prow, N.A., Hall, R.A., Petrovsky, N., Lobigs, M., 2013. JE-ADVAX vaccine protection against Japanese encephalitis virus mediated by memory B cells in the absence of CD8(+) T cells and pre-exposure neutralizing antibody. J. Virol. 8, 4395.

Lauer, P., Hanson, B., Lemmens, E.E., Liu, W., Luckett, W.S., Leong, M.L., Allen, H.E., Skoble, J., Bahjat, K.S., Freitag, N.E., Brockstedt, D.G., Dubensky, T.W., 2008. Constitutive activation of the PrfA regulon enhances the potency of vaccines based on live-attenuated and killed but metabolically active *Listeria monocytogenes* strains. Infect. Immun. 76 (8), 3742.

Layton, R.C., Petrovsky, N., Gigliotti, A.P., Pollock, Z., Knight, J., Donart, N., Pyles, J., Harrod, K.S., Gao, P., Koster, F., 2011. Delta inulin polysaccharide adjuvant enhances the ability of split-virion H5N1 vaccine to protect against lethal challenge in ferrets. Vaccine 29 (37), 6242.

Lobgis, M., Pavy, M., Hall, R.A., Lobgis, P., Cooper, P., Komiya, T., Toriniwa, H., Petrovsky, N., 2010. An inactivated vero cell-grown Japanese encephalitis vaccine formulated with Advax, a novel inulin-based adjuvant, induces protective neutralizing antibody against homologous and heterologous flaviviruses. J. Gen. Virol. 91, 1407.

Mainou-Fowler, T., MacGowan, A.P., Postlethwaite, R., 1988. Virulence of *Listeria* spp.: course of infection in resistant and susceptible mice. J. Med. Microbiol. 27 (2), 131.

Mohamed, W., Sethi, S., Tchatalbachev, S., Darji, A., Chakraborty, T., 2012. Protective immunity to *Listeria monocytogenes* infection mediated by recombinant *Listeria innocua* harboring the VGC locus. PLoS One 7 (4), e35503.

Nielsen, M., Lundegaard, C., Worning, P., Lauemøller, S.L., Lamberth, K., Buus, S., Brunak, S., Lund, O., 2003. Reliable prediction of T-cell epitopes using neural networks with novel sequence representations. Protein Sci. 12 (5), 1007.

Pamer, E.G., 2004. Immune responses to *Listeria monocytogenes*. Nat. Rev. Immunol. 4, 812.

Peña-Sagredo, J.L., Hernández, M.V., Fernandez-Llanio, N., Giménez-Ubeda, E., Muñoz-Fernandez, S., Ortiz, A., Gonzalez-Gay, M.A., Fariñas, M.C., Biobadaser group, 2008. *Listeria monocytogenes* infection in patients with rheumatic diseases on TNF-alpha antagonist therapy: the Spanish Study Group experience. Clin. Exp. Rheumatol. 26 (5), 854.

Pérez-Trallero, E., Zigorraga, C., Artieda, J., Alkorta, M., Marimón, J.M., 2014. Two outbreaks of *Listeria monocytogenes* infection, Northern Spain. Emerg. Infect. Dis. 20 (12), 2155. http://dx.doi.org/10.3201/eid2012.140993.

Peters, B., Sette, A., 2005. Generating quantitative models describing the sequence specificity of biological processes with the stabilized matrix method. BMC Bioinformatics 31 (6), 132.

Petrovsky, N., Larena, M., Siddharthan, V., Prow, N.A., Hall, R.A., Lobigs, M., Morrey, J., 2013. An inactivated cell culture Japanese encephalitis vaccine (JE-ADVAX) formulated with delta inulin adjuvant provides robust heterologous protection against West Nile encephalitis via cross-protective memory B cells and neutralizing antibody. J. Virol. 18, b10324.

Pion, M., Serramia, M.J., Diaz, L., Bryszewska, M., Gallart, T., Garcia, F., Gomez, R., de la Mata, F.J., Muñoz-Fernandez, M.A., 2010. Phenotype and functional analysis of human monocytes-derived dendritic cells loaded with a carbosilane dendrimer. Biomaterials 31, 8749.

Poulsen, K.P., Faith, N.G., Steinberg, H., Czuprinsky, C.J., 2011. Pregnancy reduces the genetic resistance of C57BL/6 mice to *Listeria monocytogenes* intragastric inoculation. Microb. Pathog. 50 (6), 360.

Rey-Ladino, J., Ross, A.G.P., Cripps, A.W., 2014. Immunity, immunopathology, and human vaccine development against sexually transmitted *Chlamydia trachomatis*. Human Vaccines Immunother. 10 (9), 2664.

Rodriguez-Del Rio, E., Marradi, M., Calderon-Gonzalez, R., Frande-Cabanes, E., Penades, S., Petrovsky, N., Alvarez-Dominguez, C., 2015. A gold-glyconanoparticle carrying a listeriolysin o peptide and formulated with Advax™ delta inulin adjuvant induces robust T-cell protection against *Listeria* infection. Vaccine 33 (12), 1465. http://dx.doi.org/10.1016/j.vaccine.2015.01.062.

Saade, F., Honda-Okubo, Y., Trec, S., Petrovsky, N., 2013. A novel hepatitis B vaccine containing Advax™, a polysaccharide adjuvant derived from delta inulin, induces robust humoral and cellular immunity with minimal reactogenicity in preclinical testing. Vaccine 31 (15), 1999. http://dx.doi.org/10.1016/j.vaccine.2012.12.077.

Sidney, J., Assarsson, E., Moore, C., Ngo, S., Pinilla, C., Sette, A., Peters, B., 2008. Quantitative peptide binding motifs for 19 human and mouse MHC class I molecules derived using positional scanning combinatorial peptide libraries. Immunome Res. 4, 2. http://dx.doi.org/10.1186/1745-7580-4-2.

Skoberne, M., Geginat, G., 2002. Efficient in vivo presentation of *Listeria monocytogenes* derived CD4 and CD8 cell epitopes in the absence of IFN-γ. J. Immunol. 168, 1854.

Stephenson, K.E., Neubauer, G.H., Reimer, U., Pawlowski, N., Knaute, T., Zerweck, J., Korber, B.T., Barauch, D.H., 2015. Quantification of epitope diversity of HIV-1-specific binding antibodies by peptide microarrays for global HIV-1 vaccine development. J. Immunol. Methods 416, 105.

Vacas-Cordoba, E., Pion, M., Rasines, B., Filippini, D., Komber, H., Ionov, M., Bryszewska, M., Appelhans, D., Muñoz-Fernandez, M.A., 2013. Glycodendrimers as new tools in the search for effective anti-HIV DC-based immunotherapies. Nanomedicine 9 (7), 972.

Valero, F.P., Rafart, J.V., 2014. Incidence study of listeriosis in Spain. Gac. Sanit. 28 (1), 74. http://dx.doi.org/10.1016/j.gaceta.2013.03.004.

Wood, L.M., Paterson, Y., 2014. Attenuated *Listeria monocytogenes*: a powerful and versatile vector for the future of tumor immunotherapy. Front. Cell. Infect. Microbiol. 4, 51. http://dx.doi.org/10.3389/fcimb.2014.00051. eCollection 2014.

Yu, K., Petrovsky, N., Schönbach, C., Koh, J.Y., Brusic, V., 2002. Methods for prediction of peptide binding to MHC molecules: a comparative study. Mol. Med. 8 (3), 137.